Guha *et al.*
Journal of Engineering and Applied Science (2023) 70:72
https://doi.org/10.1186/s44147-023-00242-4

Journal of Engineering and Applied Science

RESEARCH Open Access

Application and validation of machine vision inspection for efficient in-process monitoring of complex biomechanical device manufacturing

Bikash Guha[1*], Sean Moore[1] and Jacques M. Huyghe[1,2]

*Correspondence:
Bikash.Guha@ul.ie

[1] School of Engineering, University of Limerick, Limerick V94 T9PX, Ireland
[2] Eindhoven University of Technology, 5600 MB Eindhoven, the Netherlands

Abstract

A technique is presented for shifting the manufacturing quality control of complex biomechanical catheters away from destructive testing of finished parts. This technique uses a more efficient real-time in-process monitoring through the application of machine vision inspection of patient critical quality parameters. The approach acknowledges the challenge of this industry operating in a strict regulated environment. The higher standards of built-in quality are achieved by developing automated inspection solutions that are more accurate and repeatable. Machine vision system and associated inspection job tools are developed and used to detect defects at crucial stages of manufacturing. The vision system is then tested for its robustness using a statistical approach to ensure its measurement capability is within the allowable process range and tolerances. The integrated solution developed is proven to be robust and highly precise in maintaining the manufacturing process stable. It enabled the manufacturing process to move away from a destructive double sampling plan with a standard LTPD of 5% to an otherwise real-time 100% non-destructive verification of units. This technique provides an alternative to otherwise cost-inefficient quality control inspections utilized in regulated manufacturing environment. It gives confidence to these conservative industries to move towards adopting digital manufacturing and Industry 4.0 practices.

Keywords: Machine vision inspection, Stent delivery catheters, Measurement system analysis, Industry 4.0

Introduction

The coronary drug-eluting stents (DES) and stent delivery catheters (SDC) have been categorized as class III medical devices, i.e., a device that poses the highest risk to patient's safety as per US Food and Drug Administration (FDA) [1]. The global cardiovascular stent market has been projected to grow at a compounded annual growth rate (CAGR) of 3.8% over the period of next 5 years [2]. The catheters are complex device in themselves, and manufacturing of these high-volume devices must comply with tight tolerances to avoid damage to the patient's blood vessels while these devices are steered

into position during an angioplasty procedure [3]. Maintaining high quality and manufacturing standards are an utmost priority and extremely difficult given the high volumes. A central issue in ensuring quality of these devices is the industry being regulated in nature hinders the readily adoption of new age technologies. Any drawback of these technologies would mean a huge cost setback, damage to the brand reputation, and, in extreme cases, forcing for product recalls or banning of these products by the regulators. Facing the twin challenge of high quality and high volume, the industry is forced to shun manual processes and cautiously adopt more automation, digital manufacturing, and Industry 4.0 practices. It is a key challenge for the industry which is otherwise known to have a conservative outlook in embracing new technologies. As a result, the industry lags far behind the current digital manufacturing curve meaning product manufacturing and inspections are still predominantly manual.

This paper attempts to bridge one such gap within the quality control aspect in manufacturing of these devices. The manufacturers have till date clung to the almost a century-old end of line, acceptable sampling methods. It is partly due to either destructive nature of the tests and mainly business conservatism and hesitancy in adopting new technologies [4]. FDA suggests the manufacturers to have extensive understanding of their processes and critical product and process parameters along with the ability to control processes through quality systems and strive for continuous improvement [5]. It continues to emphasize the need for industries to move away from classical batch release and control strategies towards real-time release testing (RTRT) through utilization of process analytical technologies and tools (PAT) [6]. FDA and other international bodies have also established regulations and guidance where automated process or automated PAT have been deployed within the manufacturing process. As per its Code for Federal Regulations (CFR) Title 21 part 11—Electronic Records; Electronic Signatures—scope and application provide guidance on maintaining records and information in an electronic format [7]. It further states that for computerized systems, the agency intends to exercise enforcement discretion regarding specific requirements for validation of these systems. Title 21 CFR part 820—Quality System regulation Chapter I subchapter H—Medical Devices (21 CFR Part 820.70(i)) [8] specifically applies to automated processes. It states that "When computers or automated data processing systems are used as part of production or the quality system, the manufacturer shall validate computer software for its intended use according to an established protocol. All software changes shall be validated before approval and issuance. These validation activities and results shall be documented." The International Society for Pharmaceutical Engineering under a technical subcommittee Good Automated Manufacturing Practice (GAMP) is the golden standard for manufacturing and users of automated systems in regulated industries such as pharma or medical devices [9, 10].

The aim for this research is to develop a non-contact non-destructive vision inspection system for the inspection of patient critical parameters of catheter manufacturing process. The system is validated to the stringent requirements of statistical measurement system analysis (MSA) to guarantee system's robustness to natural process variation, a regulatory requirement for deploying PAT. A head-to-head comparison of the measurement results from the developed system is also made to the results obtained from current standard measurement techniques.

Machine vision inspection is nothing very new in the manufacturing space. Over the last decade or so, it has found application in almost all manufacturing environments, especially within high volume manufacturing such as electronic industry [11, 12], additive manufacturing [13], remanufacturing industry [14], and general manufacturing applications [15–17]. Catheter manufacturing, however, has seen very limited application of machine vision inspection, given the associated complications of operating within the regulated environment. Evidence of vision inspection application as a PAT within this industry has been so far very limited and scarce [3]. During review of academic literature, international patents and commercially available systems, very limited information is available for such vision system applications. A systematic attempt, therefore, has been made to develop and validate a vision inspection system for carrying out automatic inspection of catheter tip post laser bonding process. The novelty of this research lies in developing the automated system and proving its robustness as per the stringent standards of regulatory bodies.

Catheter tip welding, specifications, and testing

An important step of the catheter manufacturing process is the tip welding. The catheter tip welds together the inner to the balloon along with the tip. The tip is formed by a laser bonding process on a semi-automated cell. During the welding process, the polymer components supported over a metallic mandrel, are heated to create a local melt pool. The heat is created via concentrating the laser spot on the intended region with the heat being constrained over by a heat shrink tubing. Post welding, a distinct bonded tip is outputted with some typical post bonding features as shown in Fig. 1, namely, tip past inner, tip inner overlap, balloon waist inner weld, lesion entry profile diameter, and unbonded length. The specifications of these features are 1 ± 0.6 mm for balloon waist inner weld bond length, 0.350–5 mm for lesion entry profile diameter, 1 mm to 3.5 mm for tip inner overlap bond length, 0.5 to 5 mm for unbonded length, and 0.40 to 3 mm for tip past inner length (note: some specification data has been altered deliberately to protect proprietary information).

Post weld testing of the bond includes primarily destructive tensile test where the part is held in between jaws of a standard tensile tester and put to tensile stress to determine the tensile strength of the bonded components. Classical double-sampling plan are put

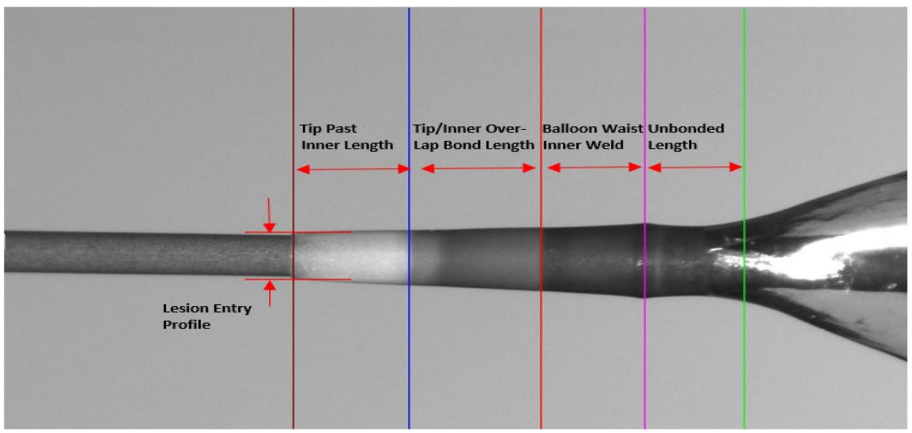

Fig. 1 Catheter tip post weld bond specifications

in place with a standard Lot Tolerance Percent Defective (LTPD) rate of 5% for batch release activities. As part of the developing this new PAT for post bond testing of the components, regression analysis and correlation studies were done to establish relation between typical post bond features to the tensile strength. When new non-contact vision system is deployed, an indirect indicative approximation can be made on the bond strengths based on the precise and accurate measurement of post weld bond features.

Test cell design and optics

A test rig is constructed to assemble the various components needed to develop the overall vision inspection system as shown in Fig. 2. The system consists of a Cognex Insight Micro 8402 camera with C-mount lens with an optical focal length of 17.526 mm lens [18]. It has adjustable/locking focus and f-stop, associated lighting (2 red front lights and 1 back light), and a blue strobe or spotlight. The lens is fitted onto the camera with a 35-mm spacer to adjust the lens working distance. The C-mount lens is chosen to provide the required field of view within the physical constraints of the inspection area.

The camera is a high-speed high-resolution monochrome and color-capable complementary metal-oxide semiconductor (CMOS) sensor with a resolution of 1600×1200 pixels. The CMOS sensor size is 9 mm diagonal, 4.5×4.5 μm sq. pixels [19]. The hierarchical organization within the vision sensor consists of three layers. The first layer is the system level where all the system parameters are stored common to all the inspections. These parameters affect the overall behavior of the vision system rather than that of a particular inspection. The second layer is then that of a product level. The product level parameters are directly associated with an inspection and affects a whole inspection that the sensor is performing. The third layer is the tool level. The tool parameters set by the user perform part of an inspection. It is at this level where all parts of the inspection are defined [20].

The inspection requires back lighting for measuring part feature outside diameter (OD) and front lighting for bond edge illumination. Strobe light-emitting diodes (LED) are chosen for light output stability driven by a strobe light controller. The strobe duration times are set as short as reasonably possible (few milliseconds) to limit vibration and ambient lighting impact on the inspection and long enough to achieve the required illumination on the part. Red front lights are found to provide the best composite contrast for all the required bond edges. The front lights are located on the tip side of the balloon, as far forward and close to the part as possible, given the constraints of the mechanical test cell layout. Two lights are used to increase illumination and reduce the sensitivity of the inspection to part variation.

Custom inspection job files

For catheter tip inspection, custom scripts (inspection job files) are developed to perform specific inspection tasks as shown in Fig. 3. The control of the test cell is governed by Visual Basic Application (VBA) which also dictates the vision inspection run sequence.

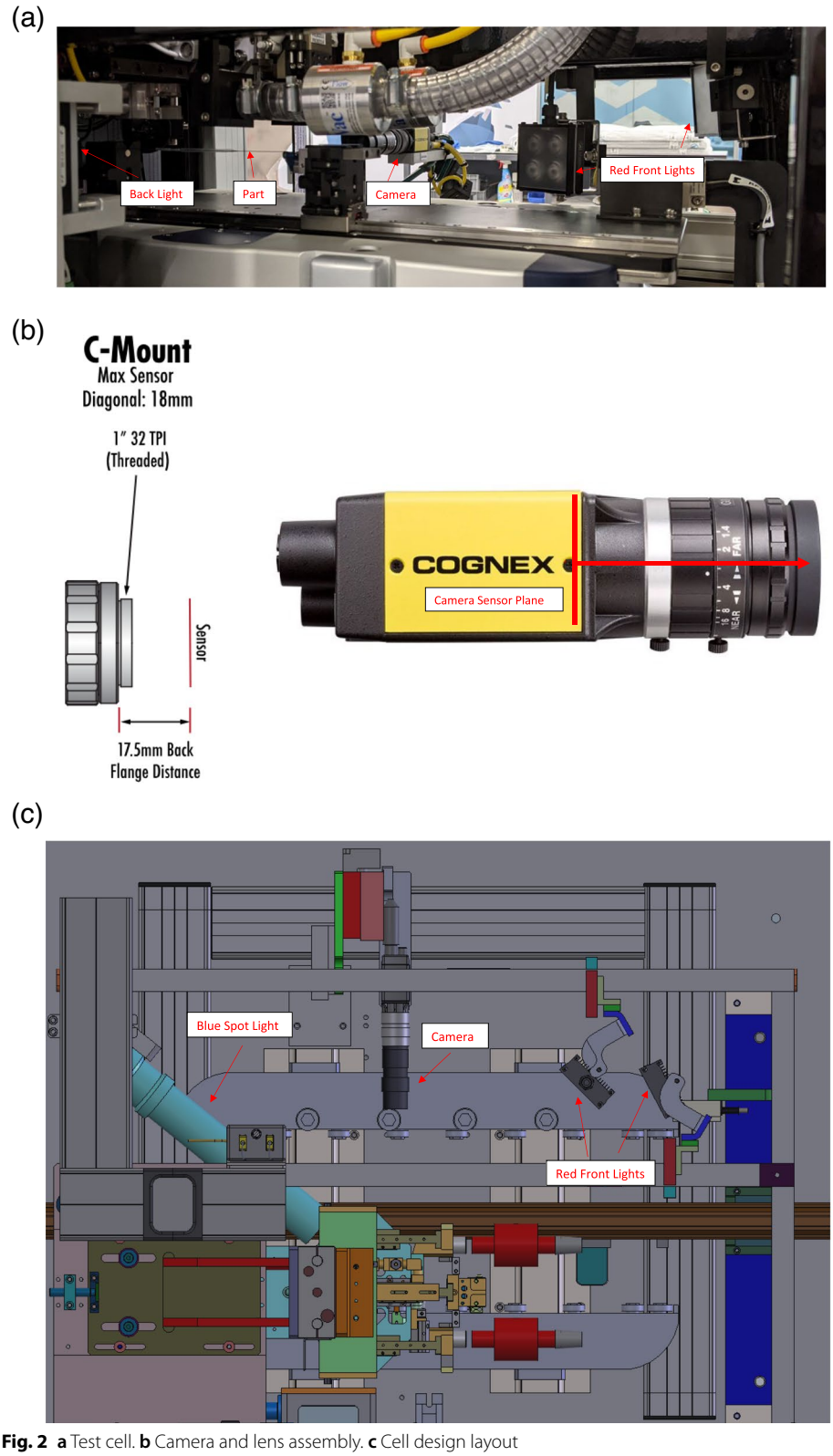

Fig. 2 **a** Test cell. **b** Camera and lens assembly. **c** Cell design layout

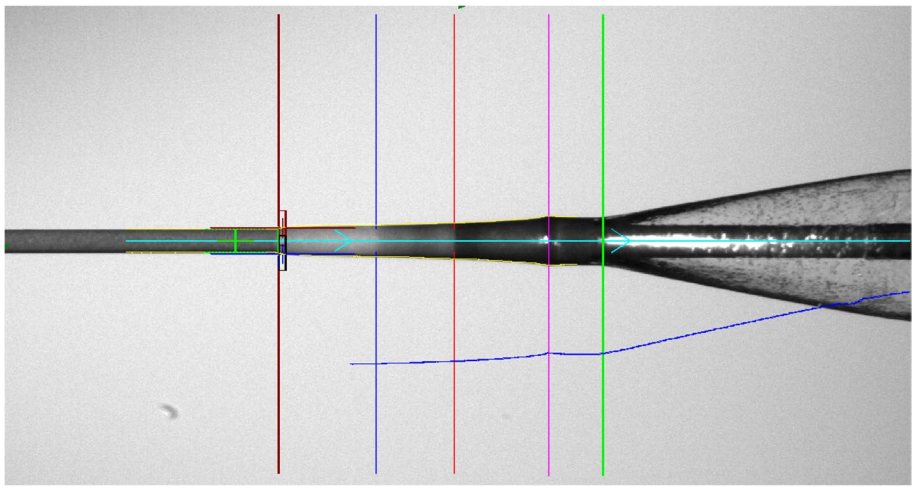

Fig. 3 Vision inspection tool script inspection results

The below list details in brief the different scripts developed to carry out tip inspection as per the product design specifications in the format Tool Name – Inspection Output – Description of the tool. Figure 3 is the culmination of all the different scripts as indicated below and also other sub-scripts that run in parallel to generate appropriate results for the main scripts.

1. Part Profile – N/A—The outside diameter (OD) of the entire part is measured, providing edge profile data for subsequent inspection tools. This measurement tool covers the entire image.
2. Vertical—Part Position Y value, Heat Shrink presence, Part presence—Finds the vertical Y location and diameter of the mandrel at the far-left edge of the image. The OD is used to determine if the heat shrink has been removed.
3. Find Tip—Find part Tip horizontal position—This tool searches along the mandrel from left to right to find the leading (distal) edge of the tip.
4. Mandrel at Tip—Find part vertical position Y value for inspection tool placement at Tip—Finds the vertical Y location and diameter of the distal mandrel left of the Tip edge. The OD and position are used to precisely place edge tools for measuring the tip lead in.
5. Tip Bond—Find part Tip Bond horizontal position—This tool searches along the Tip from left to right to find the leading (distal) edge of the tip bond.
6. Mid Bond Edge—Find part Mid Bond horizontal position—This tool searches along the Bumper Tip from left to right to find the leading (distal) edge of the Mid bond.
7. Bump OD—Max OD value—This script is designed specifically to find a convex curvature in the OD profile of a part. The lack of a weld bump suggests a possible cold weld and a weak bond.
8. Balloon Cone Trans—Finds the *X*-axis location of the balloon cone transition—This script is designed specifically to find the transition point of the maximum slope change in the OD profile of a part. The maximum slope change in the edge profile occurs at the beginning of the balloon cone.

9. Min OD – Finds the *X*-axis location and minimum diameter of the part between the bump position and balloon cone—This tool extracts OD values from the Part Profile edge data to find the minimum OD value. The tool searches the data from left to right, beginning at the Bump maximum OD position and searching into the balloon cone area.
10. Tip Bttm, Tip Top, Tip Lead In OD—Tip OD value—Tip Bottom—This tool searches a narrow area from left to right, along the bottom half of the mandrel at the tip location, to precisely locate the bottom edge of the tip. Tip Top: This tool searches a narrow area from left to right, along the top half of the mandrel at the tip location, to precisely locate the top edge of the tip. Tip Lead In OD: This tool checks for valid edge data from the lead in edge find tools and calculates the Lead-In OD measurement and displays the OD value.
11. Intensity—Intensity Avg BL, Intensity Left FL, Intensity Right FL—This tool measures the image intensities on the part and the in the background. These are light intensities from the backlight and the two red front lights.

System calibration

The proposed vision system test rig is calibrated using a custom built standardized 3 mm x 3 mm glass reticule fixture (see Fig. 4) placed within the field of view (FOV) of camera. The focus is adjusted using the adjustment rails on the rig and camera lens internal focus. The exposure of the camera system is set to default 8 ms for the purpose of calibration.

A custom calibration visual basic script is run on the system PC that generates a calibration window on screen. The aim is to fit the calibration square on the reticule within the calibration window generated until crosshairs on the corners of the window turn green confirming the FOV is set correctly (see Fig. 5a).

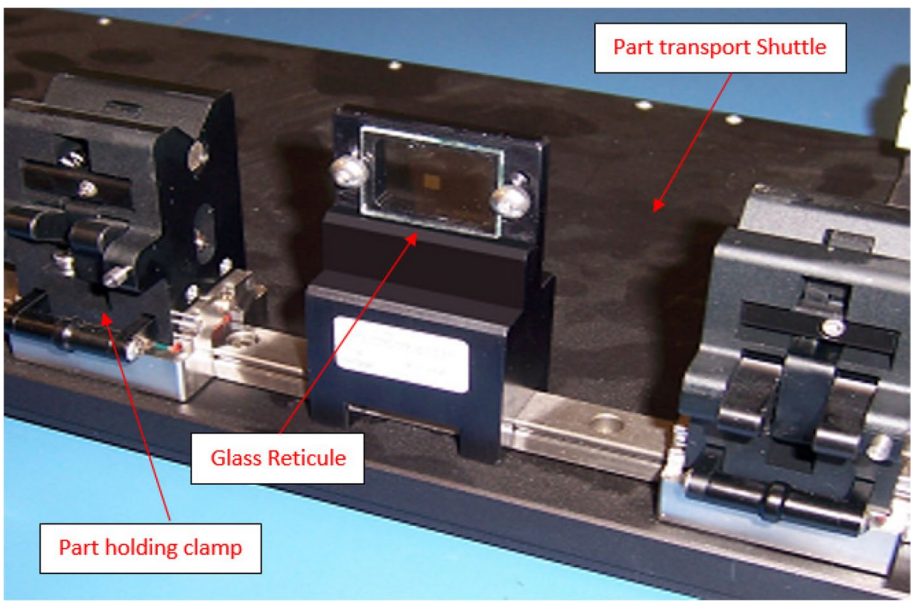

Fig. 4 Calibration fixture

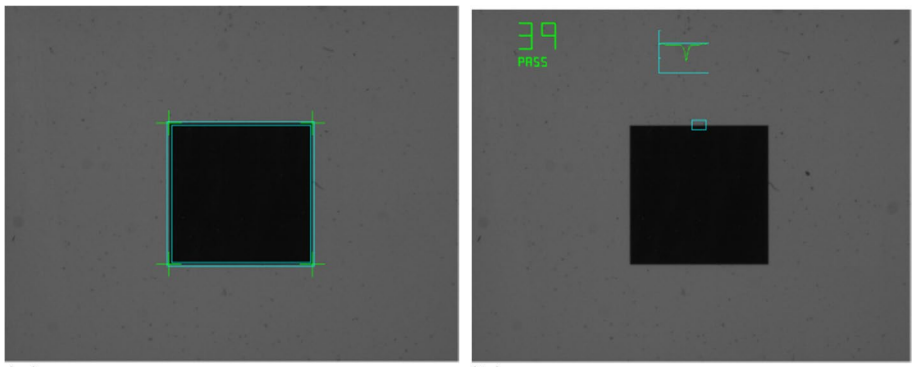

Fig. 5 **a** FOV correction. **b** Edge gradient tuning

The process is repeated to achieve the highest edge gradient with a similar window appearing on the edge of the square and fine tuning the system till the highest edge gradient is achieved and the software prompting the user with a pass notification (see Fig. 5b).

On completion of both tasks, the values are saved on the system. The script running in the background records a corresponding mm to pixel ratio on the camera memory. That figure is used every time the camera measures a feature on screen in terms of number of pixels and a corresponding measurement value in mm gets stored in the recording database.

Measurement system analysis

For systems designed to carry out 100% inspections of critical patient safety parameters, it is required to prove out the measurement system's capability in being able to carry out the job satisfactorily. Industry standard to accomplish this is through measurement system analysis (MSA). The objective of MSA is to determine how much of the total variability observed in the process is due to measurement error and to establish if the measurement system variability is acceptable and within the consumer's risk appetite.

The total variability of the parts measured are always increased by the measurement system [21] and is given by:

$$\sigma_T^2 = \sigma_{pv}^2 + \sigma_{ms}^2 \tag{1}$$

where σ_{pv}^2 is process variation arising from production process, material, machine, process environment, and operator training, and σ_{ms}^2 is measurement system variation or variation due to gage [22]. MSA determines the error in measurement which can be further classified in two categories: accuracy and precision [23]. Accuracy is the ability to produce on target results (difference between measured value and reference value) whereas precision is the ability to produce consistent results (dispersion between measured values). Table 1 shows the various components of the measurement error.

Numerically, the computation of errors of measurements can be determined as follows:

Bias for individual measurement can be given by:

$$B_{ij} = x_{ij} - R_i \tag{2}$$

Table 1 Components of measurement error in MSA

Accuracy	Precision
Bias: Accuracy of measured value compared to reference value *Linearity*: Accuracy of measured value through expected range of readings *Stability*: Accuracy of measured values over time	*Repeatability*: Ability to produce same measured value in repeated measurements by the same appraiser *Reproducibility*: Ability to get same measured value by different appraisers

where B_{ij} is the bias for jth replication of the part i, x_{ij} is the individual measurement value for jth replication of the part i, and R_i is the reference value for part i.

Average bias for n readings of an individual part can be given by:

$$\overline{B}_i = \frac{\sum_{ij=1}^{n_i} B_{ij}}{n_i} \tag{3}$$

For linearity, first, a regression line is plotted between the individual bias and reference values. The equation of the line is given by:

$$\overline{B}_i = mR_i + c \tag{4}$$

where m is the slope of the line, and c is the intercept. m and c thereafter are given by:

$$m = \frac{\sum RB - \left(\frac{1}{ab}\sum R \sum B\right)}{\sum R^2 - \frac{1}{ab}\left(\sum R\right)^2} \tag{5}$$

$$c = \overline{\overline{B}} - m\overline{R} \tag{6}$$

where a is no. of subgroups, and b is the subgroup size.

Ideal scenario would have slope m equal to zero meaning the bias is same at all reference values. In practice, there is always some bias because of the within system variation. For determining if the slope m is significantly different from zero, *t-statistic* is calculated and p-value associated with the *t-statistic* is determined. The *t-statistic* is given by

$$t = \frac{\frac{|m|}{s}}{\sqrt{\sum \left(R - \overline{R}\right)^2}} \tag{7}$$

where s is the standard deviation given by:

$$s = \sqrt{\frac{\sum B^2 - c\sum B - m\sum (R * B)}{ab - 2}} \tag{8}$$

Once the regression line has been established, confidence limits, bounds, or intervals around the regression line is determined. Confidence interval is "*the interval between two statistics that includes the true value of parameter with some probability* [24]." The equations for calculating the lower (LCB) and upper (UCB) confidence bounds (for 95% confidence interval) is given by:

$$LCB = c + mR_i - t_{(0.05,df)}s\left[\frac{1}{ab} + \frac{\left(R_i - \overline{R}\right)^2}{\sqrt{\sum\left(R - \overline{R}\right)^2}}\right]^{\frac{1}{2}} \tag{9}$$

$$UCB = c + mR_i + t_{(0.05,df)}s\left[\frac{1}{ab} + \frac{\left(R_i - \overline{R}\right)^2}{\sqrt{\sum\left(R - \overline{R}\right)^2}}\right]^{\frac{1}{2}} \tag{10}$$

Stability can only be analyzed graphically by establishing control limits and evaluating for out of tolerance conditions using normal control chart analysis. There is no specific numerical analysis or index for stability [22].

Repeatability or appraiser's agreement with themselves is given by:

$$R_{pt} = \frac{\#\ of\ appraisals\ that\ matched\ for\ i^{th}\ appraiser}{\#\ of\ appraisals\ made\ by\ the\ i^{th}\ appraiser} \times 100 \tag{11}$$

Reproducibility or agreement between appraisers is given by:

$$R_{pd} = \frac{\#\ of\ all\ appraiser^{'}\ assessment\ agree\ with\ each\ other}{\#\ inspected} \times 100 \tag{12}$$

Percent repeatability and reproducibility (%RandR), percent tolerance (%P/T), and number of distinct categories (DC) are given by:

$$\%RandR = \frac{\sigma^2_{gage}}{\sigma^2_{part}} \tag{13}$$

$$\%\mathrm{P/T} = \frac{\sigma_{gage}}{Tolerance} \times 5.15 \tag{14}$$

$$DC = \frac{\sigma^2_{part}}{\sigma^2_{gage}} \times 1.41 \tag{15}$$

where σ^2_{gage} is the standard deviation due to the gage or the measurement system, and σ^2_{part} is the standard deviation of the parts being measured. The acceptance criteria for Gage RandR (GRR) as per Automotive Industry Action Group (AIAG) standards are as below (GRR%—decision):

1. Under 10%—Generally considered to be an acceptable measurement system
2. 10%–30%—May be acceptable for some applications
3. Above 30%—Considered to be unacceptable

Number of distinct categories (Ndc), which is the smallest detectable increment between two measured values or the discrimination of the measurement resolution, is also an important factor to consider for a variable measure gage. The Ndc for a measurement system needs to be at least one tenth of the range to be measured.

Results

Once the test cell system integration is completed following amalgamation of hardware and software elements, the system is put to rigorous statistical validation testing. For this paper, the Minitab statistical software package was used to analyze the test data.

Gage linearity and bias

The test rig is first put to bias and linearity study to analyze the accuracy of the vision inspection system. Three samples from low, mid, and high end of the product size matrix are selected and measured on a master calibrated and qualified tri-axis measurement system to determine the reference values for tip past inner (TPI) length, tip inner overlap bond (IBL) length, balloon waist inner weld bond length (BL), and unbonded length (UBL). The parts are then measured on the vision system and results are fed to a statistical analysis software package Minitab for further analysis. Every part $a=3$ is measured $b=30$ times on the vision system producing $n=90$ readings which is sufficient for gage bias and linearity study as per AIAG standards [22]. Results from Minitab are as below in Table 2 and Fig. 6a–d.

Gage linearity and bias study could not be conducted for lesion entry profile diameter (EPD) for various reasons. The primary reason being EPD diameter of the catheter tip is constant across all product sizes of the catheter to be able to fit onto the guide wire and narrow blood vessels. Also, EPD is a dimensional parameter non-indicative of the tensile properties of the tip bond. This has a low-risk index as per the design failure modes and effect analysis (DFMEA) of the catheter and most of the times has other secondary downstream controls within the overall catheter manufacturing process. Nevertheless, this measurement tool has been incorporated within the vision inspection cycle to act as an additional engineering control rather than a process control and is only significant from a process yield point of view at this work step.

Gage repeatability and reproducibility

Post accuracy test, the vision inspection system is tested for precision by undertaking a Gage RandR analysis. For non-destructive tests such as these inspections, a crossed Gage RandR is recommended using the analysis of variance (ANOVA) method. Test strategy is determined wherein the smallest (2.25 mm balloon size) and the largest (4.00 mm balloon size) is selected to analyze the precision of the vision system across the operating range of the inspection system. Gage RandR matrix was created to determine number of samples, repeats, and operators as per Eq. 16; 30 is the minimum required criteria for n for crossed

Table 2 Gage linearity and bias results

Process output	Parameter	*p*-value	Null hypothesis H_o
Unbonded length	Linearity	0.370	Accept
	Average bias	0.595	Accept
Bonded length	Linearity	0.319	Accept
	Average bias	0.000	Reject
Inner bond length	Linearity	0.889	Accept
	Average bias	0.237	Accept
Tip past inner length	Linearity	0.261	Accept
	Average bias	0.840	Accept

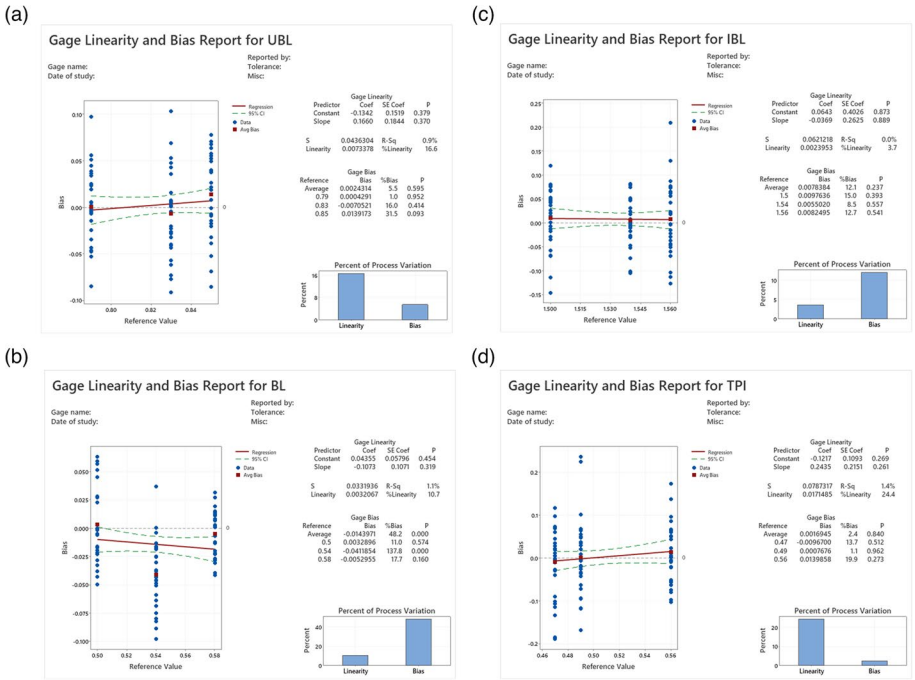

Fig. 6 Minitab reports for gage linearity and bias study for **a** UBL, **b** BL, **c** IBL, and **d** TPI

Gage RandR ANOVA accepted as per AIAG standards. Results from Minitab are as below in Tables 3, 4 and Fig. 7a-j.

$$(\#samples)x(\#operators)x(\#repeats) \geq 30(\text{minimum}) \tag{16}$$

The MSA of the developed vision system puts it under a robust statistical test that tests out the system performance under extreme operating conditions. It is to prove its consistency in measurements done at the limits of the scale and when being used by

Table 3 Gage RandR results for small balloon size

Process output	% P/T	Ndc	GRR decision	GRR report
Unbonded length UBL	22.07	1	Limited use	Figure 7a
Bonded length BL	3.18	29	Acceptable	Figure 7b
Inner bond length IBL	1.10	16	Acceptable	Figure 7c
Tip past inner TPI	9.08	4	Limited use	Figure 7d
Entry profile diameter EPD	8.67	5	Acceptable	Figure 7e

Smallest Balloon size - 2.25mm Gage RandR test summary

Table 4 Gage RandR results for large balloon size

Process output	% P/T	Ndc	GRR decision	GRR report
Unbonded length UBL	2.40	2	Limited use	Figure 7f
Bonded length BL	4.20	12	Acceptable	Figure 7g
Inner bond length IBL	3.45	3	Limited use	Figure 7h
Tip past inner TPI	12.12	2	Limited use	Figure 7i
Entry profile diameter EPD	7.92	4	Limited use	Figure 7j

Largest Balloon size - 4.00mm Gage RandR test summary

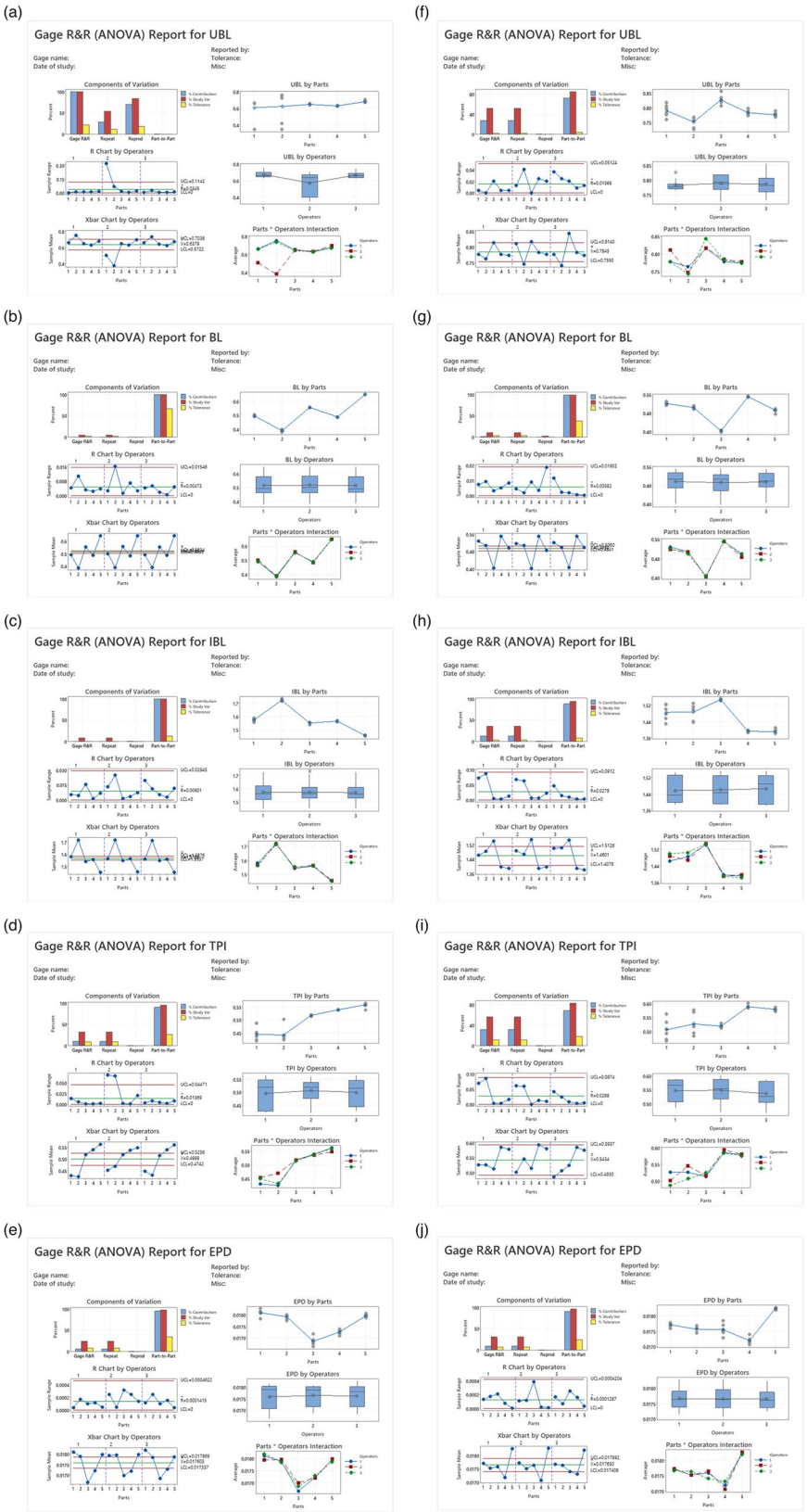

Fig. 7 Gage RandR reports for **a**–**e** small balloon size and **f**–**j** large balloon size

different personnel at different times. The test also aims to establish the reliability of the test methods developed to measure various features of the catheter bonding process. By conducting this test, it would establish the fact from a regulatory point of view that the PAT can reliably be utilized for in process inspections and that the manufacturing can move away from classical batch release testing practices.

Gage performance evaluation

To ascertain the performance of the developed system, a statistical test is performed where a sample of N units are measured on a calibrated Smartscope (see Fig. 8), and the same units are measured on the vision system over the test rig. For this test, it was determined that the measurements for inner overlap bond length (IBL) would be put to head-to-head comparison. This is the most critical of all parameters and the hardest to detect by the vision system due to the gradient transition between IBL and tip past Inner (TPI) length. First, the means of the sample size from the two measurement systems are compared using the standard statistical techniques of 2-sample *T*-test and 2-sample equivalence test. Thereafter, measurement data of each sample from standard Smartscope is compared directly with the measurement data of the same part from the vision system for a direct comparison. This is because comparing means is not always the best means of comparison for two different measurement systems [25, 26].

A power and sample size estimation were run on the Minitab software to determine number of samples needed. The statistical tests are required to have at least 80% power and 95% confidence or the *p*-value to be 0.05 [27]. The 2-sample *T*-test determines that there is no statistically significant difference in the sample mean values of the two populations. Also, a 2-sample equivalence test is conducted for determining if the sample means of the two populations are equivalent.

The historical variation or the standard deviation for the IBL measurement is 0.066 and the desired minimum detectable difference limit is set to be 0.50 mm. The

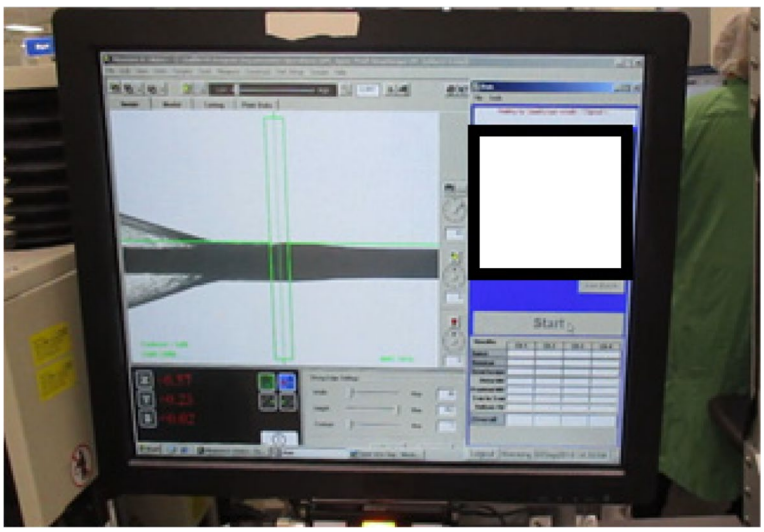

Fig. 8 Catheter tip measured manually on a Smartscope

evaluations returned that a sample size of $N = 15$ is sufficient to detect the difference of at least 0.50 mm with 100% power for the T-test and at least 0.43 mm with 80% power for the equivalence test (see Fig. 9a and b).

Prior to conducting the 2-sample T-test, the data from the sample populations are verified to have met the basic assumptions necessary for the test, namely, (i) dependent variables are continuous, (ii) measurements are independent of each other, (iii) data to be normally distributed, and (iv) equal variances in both sample populations [28, 29]. The first two assumptions are met by the nature of the experiment and data collection itself. Both sets of sample measurements are then put through Anderson–Darling normality test and are found to be normally distributed with corresponding p-values of 0.121 and 0.105 (see Fig. 9c). Thereafter, the two datasets are checked for test of equal variances. The data set passed the Levene's test with a p-value of 0.932 (see Fig. 9d), thus accepting the null hypothesis that the two sample populations have equal

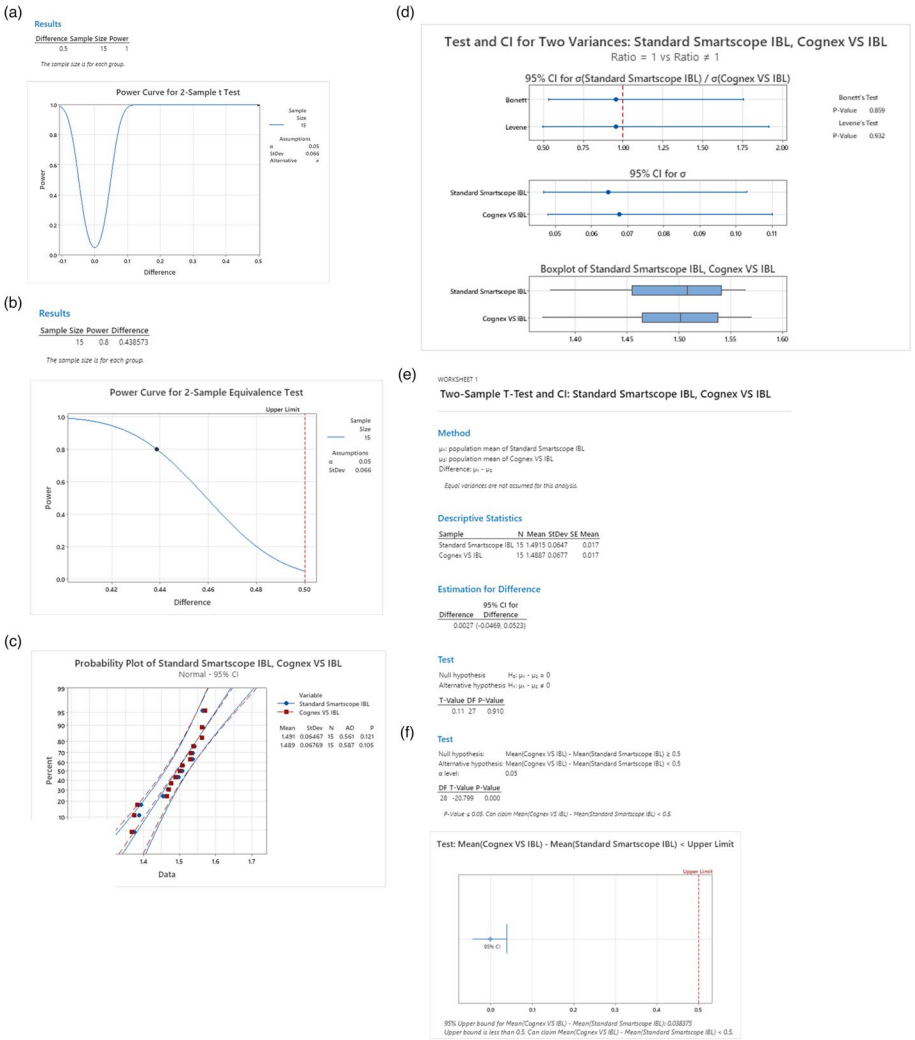

Fig. 9 **a** Power and sample size estimate for 2-sample T-test. **b** Power and sample size estimate for 2-sample equivalence test. **c** Anderson–Darling normality test. **d** Test for equal variances. **e** Results for 2-sample T-test. **f** Results for 2-sample equivalence test

variances. Having met all the assumptions, the comparison/equivalence tests are then run on the two datasets.

The results for the 2-sample T-test returned a p-value of 0.910 which is greater than the α level of 0.05 (see Fig. 9e). Therefore, the null hypothesis H_o: μ_1- μ_2= 0 is accepted for the test where μ_1 and μ_2 are the sample mean of the two populations.

The results for 2-sample Equivalence test returned a p-value of 0.0 which is less than the α level of 0.05 (see Fig. 9f). Therefore, the null hypothesis is rejected for this test which means that the alternative hypothesis of test mean μ_1 − reference mean μ_2 < 0.50 mm is accepted. This would mean that the two-sample means can be statistically deemed equivalent.

Using the graphical methods for comparing each data point, where the difference between the two measurement systems is plotted against the average of two systems, the results are found to be consistent as only one data point is outside the limits of agreement (see Fig. 10).

This is deemed to be acceptable as the difference is in order of 0.01 mm which is acceptable for the measurement type. Limitation to note for this test is that the standard Smartscope only measures up to 4 decimal places, whereas the vision system can measure up to 9 decimal places when converting pixel value to mm. The rounding effect or lack of resolution would have normalized the differences; however, it is still deemed to be not so significant for the result. The output from the automated test cell is thus considered to be at par with that of a standard measurement system.

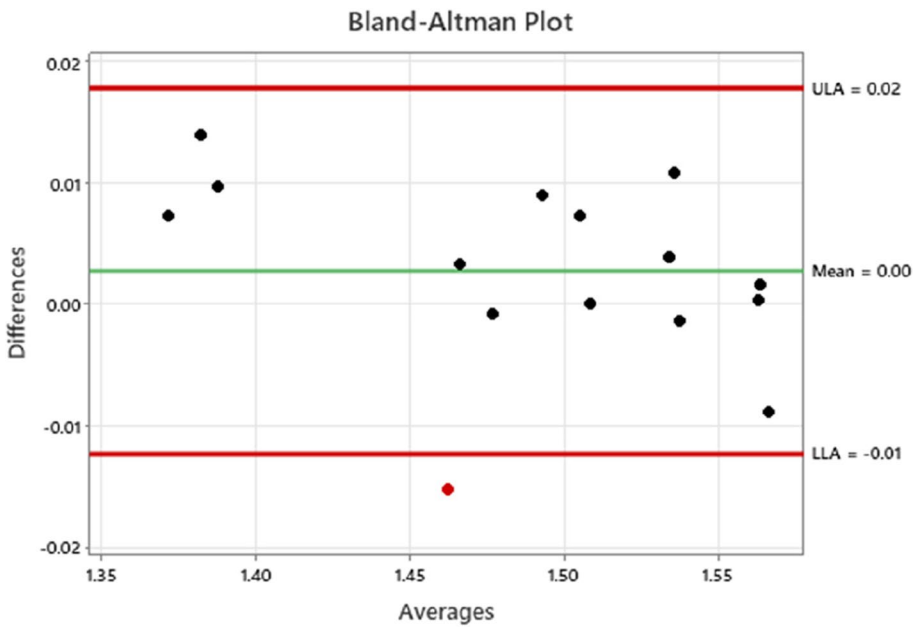

Fig. 10 Bland–Altman test on differences between two systems

Discussion

The automated vision system showed good results for gage linearity and bias for all parameters of interest except for average bias, where there is likely a potential measurement issue and warrants further investigation. For Gage RandR results, all the results for %P/T for both the extreme product sizes are acceptable. As per the industry standards, some results for Gage RandR and gage resolution restrict the system to limited use and the acceptance of which depends on the risk associated with the measured outputs or end user discretion. Furthermore, performance evaluation of the developed system against a standard measurement system is conducted, and the results are found to be consistent overall. Overall, the developed system shows promising results; however, it is recommended for more fine tuning of the inspection job files/apparatus set up if to be utilized for critical parameters such as the discussed application.

This paper has attempted to narrow down the gap that currently exists within the catheter manufacturing industry for adoption of PAT by proving with confidence that such technologies are robust and capable to meet the stringent requirements of the regulatory bodies. Very few similar attempts have been made to develop and adopt such technologies. The focus so far only has been on developing the technology but not proving its effectiveness to instill confidence for adoption. A close example would be an automated inspection system for stents [3] where the system has been developed under Matlab® in C++ using the machine vision library HALCON; however, no evidence has been provided on the repeatability/reproducibility, accuracy, and precision of the developed system. Some commercial systems that claim to have regulatory compliance 21 CFR Part 11 [30] have only attempted to inspect non-complex catheters such as urethral and intravenous with simple measurement features. A similar attempt in developing and proving system consistency was seen in an example of developing a vision inspection system for electronics failure analysis [11]. The system, however, is only attempting to find defects based on attribute features. It is not attempting to measure product feature data and testing for consistency is done on limited number of parts without a clear indication of statistical significance or reliability of the test.

Conclusions

Non-conformances in complex biomechanical catheter manufacturing is common. Traditional destructive acceptance sampling plans are not as robust and cost-efficient as 100% non-destructive machine vision inspections. This paper investigated into developing an automated vision system of critical process outputs to replace an old variable data destructive tensile testing acceptance plan. The PAT system developed is then put through rigorous statistical testing for measurement system errors to ensure the error is within permissible overall process variation. The outcome of the research is promising where the system demonstrated positive results in terms of feature detection and overall measurement variation; however, further efforts are needed to optimize the system for better resolution and expand the possibilities of the deployment to more critical applications.

This research work is one more milestone in the direction of adoption of PAT within complex biomedical device manufacturing in general. It aims to instill the confidence that highly regulated industries too can move forward towards embracing Industry 4.0 standards and practices.

Abbreviations

AIAG	Automotive Industry Action Group
ANOVA	Analysis of variance
BL	Bond length
CAGR	Compounded annual growth rate
CFR	Code for Federal Regulations
CMOS	Complementary metal-oxide semiconductor
DES	Drug-eluting stent
DFMEA	Design failure modes and effect analysis
EPD	Entry profile diameter
FDA	Food and Drug Administration
FOV	Field of view
GAMP	Good Automated Manufacturing Practice
GRR	Gage RandR
IBL	Inner overlap bond length
LCB	Lower confidence bound
LED	Light-emitting diodes
LTPD	Lot Tolerance Percent Defective
MSA	Measurement system analysis
Ndc	Number of distinct categories
OD	Outside diameter
PAT	Process analytical technologies and tools
RTRT	Real-time release testing
SDC	Stent delivery catheter
TPI	Tip past inner
UBL	Unbonded length
UCB	Upper confidence bound
VBA	Visual Basic Application

Acknowledgements
The primary author would like to acknowledge the contributions by the secondary authors, who immensely helped the article to reach to its current state by providing their precious time and valuable insights on the subject matter.

Authors' contributions
All authors have contributed to this paper. BG is the primary author responsible for drafting, literature review, and concept development. SM and JH are secondary authors for the article responsible for proof reading and peer review of the draft and getting the article submission ready. All authors have read and approved the final manuscript.

Funding
The authors declare that no funds, grants, or other support were received during the preparation of this manuscript.

Availability of data and materials
The datasets used and/or analyzed during the study is confidential in nature and available from the corresponding author on reasonable request.

Declarations

Competing interests
The authors declare no competing interests.

Received: 2 May 2023 Accepted: 14 June 2023
Published online: 05 July 2023

References

1. Kaplan AV et al (2004) Medical device development: from prototype to regulatory approval. Circulation 109(25):3068–3072. https://doi.org/10.1161/01.CIR.0000134695.65733.64
2. Lee JH, Kim ED, Jun EJ, Yoo HS, Lee JW (2018) Analysis of trends and prospects regarding stents for human blood vessels. Biomater Res 22(1):8. https://doi.org/10.1186/s40824-018-0114-1
3. Ibraheem I, Binder A (2010) An automated inspection system for stents. Int J Adv Manuf Technol 47(9–12):945–951. https://doi.org/10.1007/s00170-009-2133-5
4. Moore S. A multidimensional visualization model for zero defects in a biomechanical manufacturing environment. Doctoral Thesis, University of Limerick; 2011. Available:https://hdl.handle.net/10344/5962. Accessed: 10 Nov 2022
5. U.S. Food and Drug Administration. Quality considerations for continuous manufacturing guidance for industry. Industry Draft Guidance; 2019. p. 1–27. Available: https://www.fda.gov/Drugs/GuidanceComplianceRegulatoryInformation/Guidances/default.htm
6. U.S. Food and Drug Administration (2004) Guidance for Industry, PAT-A Framework for Innovative Pharmaceutical Development, Manufacturing and Quality Assurance. Available: http://www.fda.gov/downloads/Drugs/GuidanceComplianceRegulatoryInformation/Guidances/ucm070305.pdf

7. US FDA (2003) Guidance for Industry Part 11, Electronic Records; Electronic Signatures-Scope and Application. http://www.fda.gov/cvm/guidance/guidance.html. http://www.fda.gov/cdrh/ggpmain.html. http://www.cfsan.fda.gov/~dms/guidance.html
8. US FDA (2022) Title 21 Part 820 -Food and Drugs Chapter I-Food and Drug Administration, Department of Health and Human Services Subchapter H-Medical Devices. Available: https://www.ecfr.gov/current/title-21/chapter-I/subchapter-H/part-820?toc=1. Accessed: 08 Nov. 2022
9. International society for Pharmaceutical Engineering (2022) GAMP-5 A risk-based approach to compliant GxP computerized systems. Available: https://ispe.org/publications/guidance-documents/gamp-5-guide-2nd-edition. Accessed: 08 Nov. 2022
10. Gupta NV. A review on applications of GAMP-5 in pharmaceutical industries. Int J Drug Dev Res. 2013;5(3). Available: www.ijddr.in
11. Huang CY, Hong JH, Huang E (2019) Developing a machine vision inspection system for electronics failure analysis. IEEE Trans Compon Packaging Manuf Technol 9(9):1912–1925. https://doi.org/10.1109/TCPMT.2019.2924482
12. Edinbarough I, Balderas R, Bose S (2005) A vision and robot based on-line inspection monitoring system for electronic manufacturing. Comput Ind 56(8–9):986–996. https://doi.org/10.1016/j.compind.2005.05.022
13. Vandone A, Baraldo S, Anastassiou D, Marchetti A, Valente A (2020) 3D vision system integration on Additive Manufacturing machine for inline part inspection. Procedia CIRP 95:772–776. https://doi.org/10.1016/j.procir.2020.01.191
14. Khan A, Mineo C, Dobie G, Macleod C, Pierce G (2021) Vision guided robotic inspection for parts in manufacturing and remanufacturing industry. J Remanuf 11(1):49–70. https://doi.org/10.1007/s13243-020-00091-x
15. Häcker J, Engelhardt F, Frey DD (2002) Robust manufacturing inspection and classification with machine vision. Int J Prod Res 40(6):1319–1334. https://doi.org/10.1080/00207540110116309
16. Martinez P, Ahmad R, Al-Hussein M (2019) A vision-based system for pre-inspection of steel frame manufacturing. Autom Constr 97:151–163. https://doi.org/10.1016/j.autcon.2018.10.021
17. Gamage P, Xie SQ (2009) A real-time vision system for defect inspection in cast extrusion manufacturing process. Int J Adv Manuf Technol 40(1–2):144–156. https://doi.org/10.1007/s00170-007-1326-z
18. Hogan JP (2008) A guide to camera lens mounts. Photonics Spectra 42(4):50–53
19. Cognex (2019) 8200 and 8400 Series Vision System Specifications. https://support.cognex.com/docs/is_580/web/EN/is8000/Content/Topics/8000/Specs_8000.htm?TocPath=Specifications%7C_____1
20. Cognex (2021) Installation and User Guide for DVT Vision Sensors. https://support.cognex.com/en/downloads/insight/training/manuals
21. Mat-Shayuti MS, Adzhar SN. Measurement system analysis of viscometers used for drilling mud characterization. IOP Conf Ser Mater Sci Eng. 2017;222(1).https://doi.org/10.1088/1757-899X/222/1/012003
22. Down M, Czubak F, Gruska G, Stahley S, Benham D (2010) Measurement systems analysis. 4. 9781605342115 (ISBN)
23. Arani OM, Erdil NO (2017) Measurement system analysis in healthcare: attribute data. 67th Annual Conference and Expo of the Institute of Industrial Engineers 2017. pp 1109–114
24. Montgomery DC (1996) Introduction To Statistical Quality Control. vol. 10, no. 1. John Wiley and Sons, Inc. 9780470169926 (ISBN)
25. Altman DG, Bland JM (1983) Measurement in medicine: the analysis of method comparison studies. Available: https://www.jstor.org/stable/2987937
26. Bland JM, Altman DG (2010) Statistical methods for assessing agreement between two methods of clinical measurement. Int J Nurs Stud Elsevier Ltd 47(8):937–938. https://doi.org/10.1016/j.ijnurstu.2010.03.004
27. Bujang MA, Adnan TH (2016) Requirements for minimum sample size for sensitivity and specificity analysis. J Clin Diagn Res 10(10):01–06. https://doi.org/10.7860/JCDR/2016/18129.8744
28. Kim TK, Park JH (2019) More about the basic assumptions of t-test: normality and sample size. Korean J Anesthesiol 72(4):331–335. https://doi.org/10.4097/kja.d.18.00292
29. Schober P, Vetter TR (2019) Statistical minute two-sample unpaired t tests in medical research. Anesth Analg 129(4):911. https://doi.org/10.1213/ANE.0000000000004373
30. JLI vision (2022) Machine vision for Medical Inspection. https://info.jlivision.com/medical-inspection-brochure?utm_referrer=https%3A%2F%2Fjlivision.com%2Fvision-systems%2Fmedical-device. Accessed: 15 Nov. 2022